

H α EMISSION FROM HIGH-VELOCITY CLOUDS AND THEIR DISTANCES

M. E. PUTMAN^{1,2}, J. BLAND-HAWTHORN³, S. VEILLEUX^{4,5,6}, B. K. GIBSON⁷, K. C. FREEMAN⁸, P. R. MALONEY¹

Accepted by The Astrophysical Journal

ABSTRACT

We present deep H α spectroscopy towards several high-velocity clouds (HVCs) which vary in structure from compact (CHVCs) to the Magellanic Stream. The clouds range from being bright (~ 640 mR) to having upper limits on the order of 30 to 70 mR. The H α measurements are discussed in relation to their H I properties and distance constraints are given to each of the complexes based on $\hat{f}_{\text{esc}} \approx 6\%$ of the ionizing photons escaping normal to the Galactic disk ($f_{\text{esc}} \approx 1-2\%$ when averaged over solid angle). The results suggest that many HVCs and CHVCs are within a ~ 40 kpc radius from the Galaxy and are not members of the Local Group at megaparsec distances. However, the Magellanic Stream is inconsistent with this model and needs to be explained. It has bright H α emission and little [NII] emission and appears to fall into a different category than the currently detected HVCs. This may reflect the lower metallicities of the Magellanic Clouds compared to the Galaxy, but the strength of the H α emission cannot be explained solely by photoionization from the Galaxy. The interaction of the Stream with halo gas or the presence of yet unassociated young stars may assist in ionizing the Stream.

Subject headings: Galaxy: halo – galaxies: individual (Magellanic Stream) – galaxies: ISM, intergalactic medium – cosmology: diffuse radiation

1. INTRODUCTION

The smooth accretion of gas onto galaxies allows for continuous galaxy evolution and star formation. The intergalactic gas which feeds galaxies is seen in absorption against a bright background source along filaments of galaxies (e.g. Penton, Stocke & Shull 2002) and is predicted by simulations of the “cosmic web” (e.g. Davé *et al.* 1999). When this gas reaches a certain radius from the galaxy, it may be able to condense and cool, and in the case of our own Galaxy, the gas could become observable in 21-cm emission. Together with the remnants of Galactic satellites, these objects may be represented by the high-velocity clouds (Oort 1966).

High-velocity clouds are concentrations of neutral hydrogen which do not fit into a simple model of Galactic rotation and cover 30-40% of the sky (e.g. Wakker & van Woerden 1991; Lockman *et al.* 2002). There have been several models which propose that HVCs are the primordial building blocks of galaxies, the leftovers along the supergalactic filaments. Blitz *et al.* (1999) and Braun & Burton (1999) proposed HVCs, in particular the compact HVCs (CHVCs), represent the missing satellites of the Local Group, at mean distances of ~ 1 Mpc. These models have been called into question (e.g. Zwaan 2002; Sternberg, McKee & Wolfire 2002; Maloney & Putman 2003).

H α observations provide a direct test of whether HVCs are infalling members of the Local Group at large distances from the Galaxy. Models of the Galactic ionizing radiation field indicate that ionizing photons are capable of reaching distances on the order of 100 kpc; HVCs can act as an H I screen and the

H α emission measure reflects the ionizing photon flux reaching the cloud (Bland-Hawthorn & Maloney 1999, hereafter B99; Bland-Hawthorn & Maloney 2002, hereafter B02). This is confirmed by recent H α observations of large high velocity complexes which have direct distance bounds of < 10 kpc (Tufté *et al.* 1998; hereafter T98). If any of the HVCs are at distances on the order of 1 Mpc they should not be detectable, as the cosmic ionizing background is too low; therefore, any detection of H α emission brings the HVCs within the extended Galactic Halo. H α observations of HVCs with known distances also provide insight into how the ionizing radiation escapes from the Galactic disk, other ionization processes present in the Galactic halo, and the nature of the halo/IGM interface.

In this paper we present HVC optical line emission observations to investigate the relationship between HVCs and the Galaxy. The paper begins by summarizing the Fabry-Perot and long slit H α observations in §2, and presents the results of the observations in §3. In §4-5, we discuss our findings and interpret them in the context of the location and environment of the HVCs. The ionization of the Magellanic Stream is considered in §6 and an overview of the results is presented in §7.

2. OBSERVATIONS

The Fabry-Perot H α observations were obtained in five Anglo-Australian Telescope (AAT) observing runs from December 1997 - June 1999 and one William Herschel Telescope (WHT) run in January 1999. At both sites, the TAURUS-2 interferometer was used in conjunction with the University

¹Center for Astrophysics and Space Astronomy, University of Colorado, Boulder, CO 80309-0389; mputman@casa.colorado.edu, maloney@origins.Colorado.edu

²Hubble Fellow

³Anglo-Australian Observatory, P.O. Box 296, Epping, NSW 2121, Australia; jbh@aaopep.aao.gov.au

⁴Dept. of Astronomy, University of Maryland, College Park, MD 20742; veilleux@astro.umd.edu

⁵Cottrell Scholar of the Research Corporation

⁶Current address: 320-47 Downs Lab., Caltech, Pasadena, CA 91125 and Observatories of the Carnegie Institution of Washington, 813 Santa Barbara Street, Pasadena, CA 91101; veilleux@ulirg.caltech.edu

⁷Centre for Astrophysics & Supercomputing, Swinburne University, Mail #31, P.O. Box 218, Hawthorn, VIC, Australia 3122; bgibson@astro.swin.edu.au

⁸Research School of Astronomy & Astrophysics, Australian National University, Weston Creek P.O., Weston, ACT, Australia 2611; kcf@mso.anu.edu.au

of Maryland 44 μ m etalon. Single orders of interference were isolated using 4-cavity blocking filters with high throughput (80–90%) and bandpasses well matched to the etalon free spectral ranges. The focal plane was baffled to give either a 10' or, on the WHT (northern objects), a 5.0' field. The resulting ring pattern covered about 45 \AA ($H\alpha$, [NII] λ 6583) at the AAT and 20 \AA ($H\alpha$) at the WHT. The resolution is 1 \AA (or 46 km s $^{-1}$ at $H\alpha$). The repeated exposures were generally 10–20 minutes. A deep sky exposure was also made in a region 5 $^{\circ}$ –20 $^{\circ}$ away from the cloud, at a position that does not contain any high-velocity H I based on HIPASS limits ($< 2 \times 10^{18}$ cm $^{-2}$). The reduction and analysis is discussed in Bland-Hawthorn *et al.* (1998; hereafter B98).

HVCs and corresponding deep sky exposures were also observed with the Double Beam Spectrograph (DBS) on the Siding Spring Observatory 2.3 m telescope over 5 observing runs from August 1998 - April 2000. The DBS was set up with a 7' long slit and a slit width of 2'', yielding a spectral resolution of 0.57 \AA (26 km s $^{-1}$ at $H\alpha$). Spectral reduction was done using the VISTA and IRAF reduction packages. The two-dimensional spectra from the large sets of exposures obtained on target and sky were each reduced separately. The procedure involved bias subtraction using both bias frames and the overscan area on each exposure, flatfielding using QI lamp exposures, and cosmic ray removal with a 2.5- σ high/low filter. S-distortions and illumination effects along the slit were removed at this stage using the positions and intensity profiles of the sky lines. The central 240 rows of each 2D spectrum were extracted and then wavelength calibrated based on the positions of the sky lines in the object's spectrum (only possible with the red spectra) and the NeAr lamp spectra obtained at the same airmass as, and immediately before or after, the object's exposure. The spectra were put on an absolute flux scale using the spectra of flux standards obtained throughout the night. Each objects' exposures were added together after aligning the spectra using the closest skyline to the expected emission from the HVC as a guide. An example of a DBS spectrum is shown in Figure 1.

We examined the deep sky exposures closely for signs of $H\alpha$ emission at a velocity similar to the closest detectable H I and found no indication of emission. This was especially important to check considering the OVI that has been detected in absorption at the velocities of nearby H I HVCs, but off the H I contours of these clouds (Sembach *et al.* 2003), and the extended low H I column density emission found around cataloged HVCs (Lockman *et al.* 2002). We assume foreground Galactic extinction along a given sight line, measured from the COBE/DIRBE maps (Schlegel *et al.* 1998), and therefore correct all $H\alpha$ emission measures (E_m) for dust extinction. We also include the uncorrected E_m values in Tables 1 and 2, as the dust correction may not be realistic for the low latitude clouds. E_m upper limits quoted throughout this paper are 2-sigma for the TAURUS data and 3-sigma for the DBS data. Our characteristic detection errors are approximately 10 mR if the $H\alpha$ detection is at least 2 \AA from a skyline, but close to a skyline the errors can reach 15–30 mR. Future use of the nod+shuffle technique (Glazebrook & Bland-Hawthorn 2001) with the Fabry-Perot staring method may be able to reach levels of ~ 5 mR.

Many of the observed HVCs were first identified by HIPASS (see Putman *et al.* 2002a; hereafter P02). This is especially true of the CHVCs. The clouds observed were chosen because they have: H I velocities which isolate an equivalent velocity $H\alpha$ line from the skylines, a proposed extragalactic nature (e.g.

the CHVCs), and/or an estimate has been made of their distance and/or origin (e.g. Complex M, Magellanic Stream). In the latter case, the observations could be used to clarify the nature of the $H\alpha$ emission. Several positions observed by Weiner & Williams (1996; hereafter WW96) and T98 were repeated to compare observing and reduction methods.

3. RESULTS

The results of the observations are described in Table 1 and 2. Table 1 lists the positive detections and Table 2 the non-detections. The objects are grouped in terms of their high-velocity classification and are named either by their traditional name or by their P02 classification, which is the type of cloud (CHVC = Compact HVC, :HVC = slightly more extended than a CHVC, HVC = extended HVC, or XHVC = a HVC which has H I emission that merges with Galactic velocities), followed by the intensity weighted Galactic longitude and latitude and the central LSR velocity. The H I properties are from P02 (excluding the northern targets which are from the LDS (e.g. Complexes H and M)) and are always taken along the sightline of the $H\alpha$ observation. The results of B98, T98, and Tufte *et al.* (2002; hereafter T02) are also included in Table 1. The columns of Table 1 are: ℓ and b coordinates of the $H\alpha$ observation, HVC name, H I column density, H I velocity (LSR), H I velocity width, the extinction corrected $H\alpha$ emission measure with W or D in parentheses if the result is from WHAM or the DBS respectively, the value of the $H\alpha$ emission measure before the extinction correction, the [NII] λ 6583/ $H\alpha$ ratio, the velocity of the $H\alpha$ detection (LSR), and the predicted distance to the HVC based on its ℓ , b , and extinction corrected emission measure (see §4). Some of the [NII]/ $H\alpha$ ratios are not included due to the observation not including the wavelength of the [NII] λ 6583 line (i.e. the WHT and WHAM observations). Table 2 does not include the [NII]/ $H\alpha$ ratio or the predicted distance (see §5), but does include two limits on [OIII] emission.

The close relationship between H I velocity and $H\alpha$ velocity is shown in Figure 2 and the complete lack of correlation between the $H\alpha$ emission measure and H I column density is shown in Figure 3. This is what would be expected if the outer skin of the HVC is being ionized by an external ionizing radiation field. Figure 2 also shows that non-detections (open diamonds) span the entire range of high velocities. Though not shown, there is also no relationship between the strength of the $H\alpha$ emission and the velocity of the HVC (in the LSR or GSR reference frame). Figure 3 shows that undetected clouds span the entire range of H I column densities, i.e. there does not currently seem to be a lower or upper column density cutoff. The distribution of the $H\alpha$ detections and non-detections on the sky in Galactic coordinates is shown in Figure 4, and a large number of the $H\alpha$ observations are depicted on the H I map of the Magellanic System shown in Figure 5. We now discuss the specific detections listed in Table 1 and the undetected clouds listed in Table 2. Pictures and spectra of most of the high-velocity complexes are shown in Putman (2000).

3.1. Detections

Complexes: Several of the HVCs detected in $H\alpha$ are part of larger complexes which are defined by Wakker & van Woerden (1991). The $H\alpha$ brightest of these is Complex L, a negative velocity HVC made up of several clumpy filaments, with several small clouds scattered amongst the filaments. The cloud mapped here is HVC341.6+31.4-142 in the P02 catalog and the brightest emission lies closest to the head of the cloud. Com-

plex L has a highly elevated [NII]/H α ratio (2.7). Along with the detections there was one non-detection in a very low column density ($\sim 10^{18}$ cm $^{-2}$) part of Complex L. All of the positions with bright detections have column densities between $1.6 - 3.6 \times 10^{19}$ cm $^{-2}$.

The other detected complexes are: Complex M, which has an upper distance constraint of < 4 kpc (Ryans et al. 1997) and was detected at a similar level by T98, Complex H, which lies along the Galactic Plane making this detection more tentative (especially since the H α velocity is offset by 30 km s $^{-1}$ from the H I velocity), and Complex GCP (Smith Cloud) which was originally presented in B98 and now has a limit on the [OIII] emission at the position of Smith1 (< 70 mR; Table 2). We include the T98 detections of Complexes A and C with a model distance because they have direct distance limits of $4-10$ kpc (van Woerden et al. 1999) and > 6 kpc (Wakker 2001), respectively.

The Magellanic Stream: The Magellanic Stream shown in Figure 5 is the result of the interaction of the Large and Small Magellanic Cloud with each other and the Galaxy. It trails the Magellanic Clouds for over 100° through the South Galactic Pole and has a velocity gradient of 700 km s $^{-1}$ from head to tail (relative to the Local Standard of Rest; 400 km s $^{-1}$ relative to the Galaxy). The Stream is a complicated network of filaments and clumps, but remains relatively continuous along its entire length (see Putman et al. 2003; hereafter P03). Stars have not yet been found in the Stream (e.g. Guhathakurta & Reitzel 1998), but H α emission has been previously detected by WW96 at the level of $200 - 400$ mR.

We observed several positions along the Magellanic Stream, including one repeat of a WW96 observation, with both TAURUS and the DBS. The repeat observation of MSIIa is approximately the same as WW96 with TAURUS, but is lower with the DBS. This could be due to the difference in the field of view of TAURUS and the DBS (a $10'$ diameter FOV versus a $7' \times 2''$ slit). [NII] was also detected and the ratio to H α is low compared to the Smith Cloud and Complex L (0.15 vs. $0.6 - 2.7$). MSIIa was subsequently observed in [OIII] $\lambda 5007$ and no detection was obtained (< 52 mR; Table 2). As tabulated in Table 1, a new relatively weak H α detection was made at the head of the Stream, $(\ell, b) = 304^\circ, -67^\circ$, and at the position of the background QSO Fairall 9 where OVI absorption has also been detected ($10^{14.3}$ cm $^{-2}$; Sembach et al. 2003). There was also a non-detection at $(\ell, b) = 293.4^\circ, -56.4^\circ$ and at the tail of the Stream (MSV; $(\ell, b) = 96.5^\circ, -53.9^\circ$) as tabulated in Table 2. As shown in Figure 5, there are large variations in the strength of the H α emission along the Stream's length, and so far there does not seem to be a correlation with the H I column density (Figure 3). However, one should consider that the beam used in the H I observations is larger than the FOV of TAURUS ($15.5'$ vs. $10'$). Though the number of observations remains limited, there also does not seem to be a gradient of H α brightness along the Stream. Currently, the brightest detection is approximately at the South Galactic Pole in a region of complexity in terms of the high-velocity H I gas distribution (P03). The velocities of the H I and H α lines generally closely agree (within ~ 10 km s $^{-1}$; Figure 2). Several positions along the Magellanic Bridge and Leading Arm were also observed. All of the pointings were non-detections (see Table 2 and Figure 5), except for an extremely bright observation at the position of a known OB association (Bridge M in Table 1; see also Marcelin et al. (1985)).

Compact High-Velocity Clouds (CHVCs): Two compact

high-velocity clouds (CHVCs) were detected with the DBS. CHVC197.0-81.8-184 is located $\sim 10^\circ$ from the Stream where it passes through the South Galactic Pole (see Figure 5). The H α detection of this cloud (Fig. 1) is at the level of many of the Stream detections. The second CHVC is a very small and isolated cloud located in the region leading the LMC (Figure 5). CHVC266.0-18.7+336 has a velocity which places the H α line at the edge of a skyline, making the brightness of this detection somewhat less certain. The CHVC detections of T02 with model distances are also included in Table 1.

3.2. Non-Detections

There are several clouds which were not detected in this survey and are summarized in Table 2. Some of these clouds have detections reported in the conference proceedings of Weiner et al. (2001), but the precise coordinates of their observations have not yet been reported. This is not unusual considering the range of detections and non-detections noted in the previous section within the same high-velocity complex. Many of the HVCs which we have only non-detections for lie in approximately the same region of the sky (see Figure 4). The undetected clouds mostly lie in the Galactic Longitude range of $\ell = 250^\circ - 320^\circ$, and include the length of the Leading Arm of the Magellanic System (Figure 5), several HVCs and CHVCs, and part of the Extreme Positive Velocity Complex. We note that many of these clouds (marked with a * in Table 2) have velocities that place the H α line close to a skyline, making the non-detections somewhat less certain.

Additional non-detections include the high positive velocity cloud HIPASS J1712-64 (Kilborn et al. 2000) which has an H α upper limit of 44 mR, and the clouds associated with the Sculptor dSph galaxy by Carignan et al. (1998) (cataloged as CHVC286.3-83.5+091 and CHVC290.6-82.8+095 in P02). It is unclear if these clouds are actually associated with the Sculptor dSph. The H I maps of P03 and Carignan (1999) show the complexity of this region in high-velocity gas, with a high concentration of clouds at similar and very different velocities to the Sculptor dSph. There is an undetected negative velocity XHVC at approximately -145 km s $^{-1}$ along our observed sightline to the clouds associated with the Sculptor dSph, as well as a nearby positive velocity XHVC, which was also undetected.

4. THE H α DISTANCE CONSTRAINT

The H α distance constraint is based on photoionizing radiation escaping from the Galactic disk and ionizing the surface of H I clouds within the Galactic halo (B98). It relies on our knowing the strength and morphology of the halo ionizing field, and can be affected by a cloud's covering fraction, topology, and orientation to our line of sight (B02). Variations in H α brightness across a single HVC may be due to these issues, and we stress that the H α brightest point on the HVC (i.e. the point on the cloud receiving the most ionizing photons from our Galaxy) is the measure that should be used when estimating the HVC distance. Since we will not know if we have observed the brightest point on a particular HVC until we are able to do large scale H α mapping of each cloud, our far field distance estimates in Table 1 currently serve as upper limits. Several HVCs with strong direct distance constraints (see Wakker (2000) for a summary) have now been detected in H α by WHAM (T98), Weiner et al. (2001), and this survey. There is also an IVC (Complex K; Haffner et al. 2001) that has been completely mapped in H α emission and has a distance constraint. The H α emission measures from these clouds are consistent with the model pre-

dictions of B99 – updated in B02 to include spiral arms – which uses an escape fraction normal to the disk of $\hat{f}_{\text{esc}} = 6\%$ ($f_{\text{esc}} \approx 1 - 2\%$ averaged over 4π sr). The escape fraction used in the B02 spiral arm model has been adopted based on its agreement with the direct distance determinations and $\text{H}\alpha$ emission measures for Complex A, M, C, and the IVC, Complex K. It has a factor of two uncertainty which could affect the predicted distances listed in Table 1 by 50%. Figure 6 shows the effect of using a model with spiral arms compared to exponential and uniform disk models. The halo ionization field is very different for a dusty spiral versus an exponential disk within 10 kpc of the Galactic disk.

All of the HVCs detected in $\text{H}\alpha$ emission would be at distances within 40 kpc in the context of this model. The detection of two CHVCs indicates that some fraction of this population falls within the extended Galactic halo. This is supported by the CHVC detections of T02. These CHVCs would be within ~ 13 kpc using this distance determination method. The model prediction for a radius vector towards Complex L is shown in Fig. 7. Note that the spiral arm model predicts that Complex L lies directly over a spiral arm, but there is a near and far field solution, depending on its exact position. There is some indication that HVCs along sightlines over spiral arms are brighter, as expected for clouds within about 10 kpc (B02), but more sightlines are needed to confirm this.

Though the detection of $\text{H}\alpha$ emission argues for HVCs being within the Galactic halo, the brightness of the Magellanic Stream detections needs to be understood before the distance constraint can be considered fully reliable (see §6 and Bland-Hawthorn & Putman 2001, hereafter B01). We also note that Complex L and GCP (the Smith Cloud) not only have high $\text{H}\alpha$ emission measures (which makes sense, as they most likely lie inside the solar circle above the spiral arms), but also elevated $[\text{NII}]/\text{H}\alpha$ emission. The $[\text{NII}]$ emission may be an indication of enhanced electron temperatures (Reynolds, Haffner & Tuftes 1999), rather than the presence of an alternative source of ionization (e.g. shocks). There are a variety of ways to produce this effect (e.g. photoelectric heating (Wolfire *et al.* 1995)), and the enhanced low-ionization emission is also seen in the high latitude gas of spirals (Haffner *et al.* 1999; Veilleux *et al.* 1995; Miller & Veilleux 2003a, 2003b). In essence, we can use the elevated $[\text{NII}]/\text{H}\alpha$ to argue that some HVCs are more than several kiloparsecs from the plane, and comprise part of the extended ionized atmosphere seen in external galaxies. Further support comes from HI structure of these clouds, each of which show possible extensions into Galactic HI .

5. DO NON-DETECTIONS CORRESPOND TO LARGE DISTANCES?

If the $\text{H}\alpha$ normalization to local HVCs is valid, this may indicate that some HVCs which are faint or undetected in $\text{H}\alpha$, particularly those at high latitude, are dispersed throughout the extended halo on scales of 50 kpc or more. The cosmic ionizing background radiation ($\sim 10^4$ phot/s; Maloney & Bland-Hawthorn 1999) would correspond to a 5 mR $\text{H}\alpha$ detection and would only begin to dominate over the Galactic ionizing radiation field approximately 100 kpc from our Galaxy. Considering the $\text{H}\alpha$ upper limits in some cases and the variations in intensity across the HVCs, it remains to be seen whether most of the clouds which have non-detections are actually at large distances from the Galactic Plane. $\text{H}\alpha$ mapping across an entire HVC to find the brightest $\text{H}\alpha$ emission, higher resolution HI observations to clarify the column density at the position of the $\text{H}\alpha$

observation, and the development of models of the escape of ionizing radiation from the Galactic Plane will help resolve the non-detection issue. It may be that some clouds will remain undetected in certain directions if they lie at too low an angle from our viewpoint, or do not lie above spiral arms or HII regions. Shadowing and the size of the TAURUS beam may also be important considerations. There may be an *observed* relationship between the strength of E_m and the position of the cloud above the Galaxy, as clouds at $\ell > 330^\circ$ and $\ell < 60^\circ$ have a slight tendency to be brighter and clouds between $\ell = 250 - 320$ remain largely undetected (Figure 4). This is expected from their line of sight over the Galaxy (see Taylor & Cordes 1993) and from the B02 model.

6. WHAT IS IONIZING THE MAGELLANIC STREAM?

The Stream is brightest at the South Galactic Pole and fainter towards the head and tail. This would be expected for halo gas ionized by an opaque disk where ionizing photons escape preferentially along the Galactic poles (B99). The match between the HI velocity and the $\text{H}\alpha$ velocity for all clouds supports photoionization. However, if ionizing photons from the Galaxy are reaching HVCs at distances of ~ 10 kpc, why are Stream positions near the South Galactic Pole, which most likely lie at distances between 20 – 100 kpc (Gardiner 1999; Moore & Davis 1994), consistently brighter than the HVCs? As shown in Figure 8, at a mean Stream distance of 55 kpc, the expected emission measure of a flat HI stream is 30–50 mR (B02), an order of magnitude fainter than the brightest detections. Figure 8 also shows that the contribution from the LMC will not play a dominant role in ionizing the majority of the Stream.

Is it possible that sections of the Stream are just that much closer to the Galaxy disk than the Magellanic Clouds? With the detection of the head of the Stream (Fairall 9 sightline), this possibility seems unlikely, as the head of the Stream is presumed to be close to the Magellanic Clouds (50–60 kpc). Thus the distances predicted in Table 1 for the Stream sightlines are not relevant and we need to look for another source of ionization in the Stream. The detection of O VI absorption in and around the Stream may provide some clues (Sembach *et al.* 2003). Interaction with a halo medium could provide some pre-ionization which could elevate the Stream’s $\text{H}\alpha$. The outer halo medium may well be clumpy, particularly at the poles, from the leftovers of other satellites or from self-interaction of the Stream (B01; P03). CHVC197.0-81.8-184 may represent some of this debris. This CHVC is only 10° from the main filament of the Stream and is as $\text{H}\alpha$ bright as the Stream, possibly indicating a large spread of debris associated with Stream’s $\text{H}\alpha$ emission. Two of the T02 detected CHVCs (shown in Fig. 5) may also represent the spread of ionized Stream debris.

Another possibility is that there are stars associated with the Stream which have yet to be detected. Recent results have found small isolated HII regions in interacting systems that can be ionized by a few O stars (e.g., Gerhard *et al.* 2002; Ryan-Weber *et al.* 2003). This indicates that isolated star formation can be triggered in low density interactive debris, which could in turn play an important role in ionizing this material. A single massive O star 1 kpc from the Stream could lead to an emission measure of 40 mR. If the star was actually embedded in the Stream this contribution would obviously be much higher. White dwarfs would not significantly contribute to the ionization of the Magellanic Stream unless their density was much higher than that found in the solar neighborhood (Bland-Hawthorn, Freeman, & Quinn 1997). Thus far, only limited

areas of the Stream have been surveyed for stars. Ongoing and future stellar surveys will provide further insight into the possibility of the Stream harboring young, ionizing stars.

7. OVERVIEW

The $H\alpha$ observations presented here are a combination of detections and non-detections on clouds with $H\text{I}$ column densities greater than a few times 10^{18} cm^{-2} . This represents the complex nature of the ionized component of HVCs and the importance of mapping across an entire cloud before accepting a non-detection as meaningful for the entire high-velocity complex. The results thus far show a population of clouds which appear to extend out of Galactic $H\text{I}$ emission, are $H\alpha$ bright, and show an elevated $[\text{NII}]/H\alpha$ ratio, as well as an undetected population which tend to be in a specific region of Galactic longitude and are relatively isolated from Galactic emission. The detection of several CHVCs in both this paper and the T02 paper indicates that many of these clouds are indeed within the Galactic halo. The non-detections of some CHVCs cannot be used to argue for a greater distance until the origin of the non-detections in other complexes is understood.

The $H\alpha$ emission measures of the clouds with distance constraints are consistent with the surfaces of the clouds being ionized by $\sim 6\%$ of the Galaxy's ionizing photons. All of the clouds detected here are within 40 kpc of our Galaxy based on their level of $H\alpha$ emission. The Magellanic Stream appears to fall into a different category than the currently detected HVCs, with bright $H\alpha$ emission but little or no $[\text{NII}]$ emission, possibly due to the lower metallicities of the Magellanic Clouds compared to the Galaxy. The strength of the $H\alpha$ emission cannot be easily explained by photoionization from the Galaxy alone, and it is possible that interaction with halo debris, or the presence of yet unassociated young stars, is partially responsible for the Stream's elevated $H\alpha$ emission. Through future $H\alpha$ observations which include mapping head-tail $H\text{I}$ clouds, the length of the Magellanic Stream, OVI absorption sightlines, and complexes of known distance, and the development of models which trace the path of the escaping photons from the Galactic Plane, we may come to a consensus on the origin of the $H\alpha$ emission in all high-velocity clouds.

We thank our referees, Robert Benjamin and an anonymous reviewer, for many useful comments, and Ben Weiner and Mike Shull for helpful discussions. M.E.P. acknowledges support by NASA through Hubble Fellowship grant HST-HF-01132.01 awarded by the Space Telescope Science Institute, which is operated by AURA Inc. under NASA contract NAS 5-26555. S.V. is indebted to the California Institute of Technology and the Observatories of the Carnegie Institution of Washington for their hospitality, and is grateful for partial support of this research by a Cottrell Scholarship awarded by the Research Corporation, NASA/LTSA grant NAG 56547, and NSF/CAREER grant AST-9874973. B.K.G. acknowledges the support of the Australian Research Council, through its Large Research Grant and Discovery Project schemes.

REFERENCES

- Bland-Hawthorn, J., Veilleux, S., Cecil, G.N., Putman, M.E., Gibson, B.K. & Maloney, P.R. 1998, MNRAS, 299, 611 (B98)
- Bland-Hawthorn, J., Freeman, K.C. & Quinn, P. J. 1997, ApJ, 490, 143
- Bland-Hawthorn, J. & Maloney, P.R. 1999, ApJ, 510, L33 (B99)
- Bland-Hawthorn, J & Putman, ME. 2001. In Gas and Galaxy Evolution, ASP 240, 369, eds JE Hibbard, M Rupen, J van Gorkom (B01)
- Bland-Hawthorn, J & Maloney, PR. 2002. In Extragalactic Gas at Low Redshift, ASP 254, 267, eds JS Mulchaey & J Stocke (B02)
- Blitz, L., Spiegel, D.N., Teuben, P.J., Hartmann, D. & Burton, W.B. 1999, ApJ, 514, 818
- Braun, R. & Burton, W.B. 1999, A&A, 341, 437
- Carignan, C. 1999, PASA, 16, 18
- Carignan, C., Beaulieu, S., Cote, S., Demers, S. & Mateo, M. 1998 ApJ, 116, 1690
- Davé, R., Hernquist, L., Katz, N. & Weinberg, D. 1999, ApJ, 511, 521
- Haffner, L.M., Reynolds, R.J. & Tuftte, S.L. 2001, ApJ, 556, 33
- Haffner, L.M., Reynolds, R.J. & Tuftte, S.L. 1999, ApJ, 523, 223
- Gardiner, L.T., 1999, in Stromlo Workshop on HVCs, ASP 166, eds. Gibson, B. & Putman, M., 292
- Gerhard, O., Arnaboldi, M., Freeman, K.C., & Okamura, S. 2002, ApJ, 580, 121
- Glazebrook, K. & Bland-Hawthorn, J. 2001, PASA, 113, 197
- Guhathakurta, P. & Reitzel, D.B. 1998, in Galactic Halos: A UC- Santa Cruz Workshop, ASP 136, ed. Zaritsky, D., 22
- Kilborn, V. et al. 2000, AJ, 120, 1342
- Lockman, F.J., Murphy, E.M., Petty-Powell, S. & Urlick, V.J. 2002, ApJS, 140, 331
- Marcelin, M., Boulesteix, J. & Georgelin, Y.P. 1985, Nature, 316, 705
- Maloney, P.R. & Bland-Hawthorn, J. 1999, 522, L81
- Maloney, P.R. & Putman, M.E. 2003, ApJ, 589, 270
- Mathewson, D.S., Schwarz, M.P. & Murray, J.D. 1977, ApJ, 217, 5
- Miller, S. T. & Veilleux, S. 2003a, ApJS, 148, 000 (astro-ph/0305026)
- Miller, S. T. & Veilleux, S. 2003b, ApJ, 592, 000 (astro-ph/0304471)
- Moore, B. & Davis, M. 1994, MNRAS, 270, 209
- Oort, J.H. 1966, Bull. Astron. Inst. Neth., 18, 421
- Penton S., Stocke, J. & Shull, J.M. 2002, ApJ, 565, 720
- Putman, M.E. 2000, Ph.D Thesis, Australian National Univ.
- Putman, M.E. et al. 2002, AJ, 123, 873 (P02)
- Putman, M.E., Staveley-Smith, L., Freeman, K.C., Gibson, B.K. & Barnes, D.G. 2003, ApJ, 586, 170 (P03)
- Reynolds, R.J., Haffner, L.M. & Tuftte, S.L. 1999, ApJ, 525, L21
- Ryans, R.S.I. et al. 1997, MNRAS, 289, 83
- Ryan-Weber, E., Meurer, G., Freeman, K.C., Putman, M.E., Webster, R. et al. 2003, ApJ, submitted
- Schlegel, D.J., Finkbeiner, D.P. & David, M. 1998, ApJ, 500, 525
- Sternberg, A., McKee, C.F. & Wolfire, M.G. 2002, ApJS, 143, 419
- Sembach, K. et al. 2003, ApJS, 146, 165
- Taylor, J.H. & Cordes, J.M. 1993, ApJ, 411, 674
- Tuftte, S.L., Reynolds, R.J. & Haffner, L.M. 1998, ApJ, 504, 773 (T98)
- Tuftte, S.L., Wilson, J.D., Madsen, G.J., Haffner, L.M. & Reynolds, R.J. 2002, ApJ, 572, 153 (T02)
- van Woerden, H. et al. 1999, Nature, 400, 138
- Veilleux, S., Cecil, G.N. & Bland-Hawthorn, J. 1995, ApJ, 445, 152
- Wakker, B. 2001, ApJS, 136, 463
- Wakker, B. & van Woerden, H. 1991, A&A, 250, 509
- Weiner, B.J. & Williams, T.B. 1996, AJ, 111, 1156 (WW96)
- Weiner, B.J., Vogel, S.N. & Williams, T.B. 2001, In Gas and Galaxy Evolution, ASP 240, 515, eds JE Hibbard, M Rupen, J van Gorkom
- Wolfire, M.G. et al. 1995, ApJ, 453, 673
- Zwaan, M. 2002, MNRAS, 325, 1142

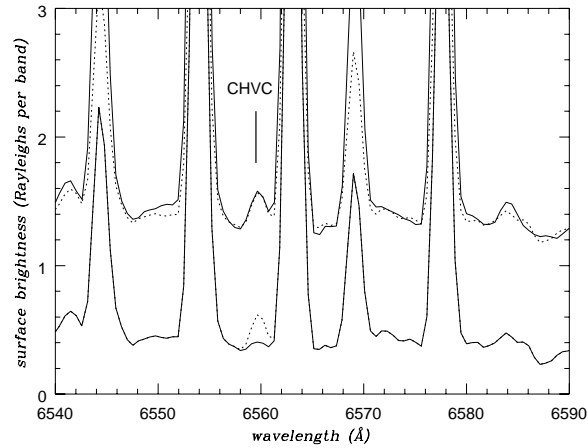


Fig. 1. DBS spectrum of CHVC197.0-81.8-184 showing $H\alpha$ emission at the level of 220 mR. The top spectrum is the CHVC observation (solid line) with the sky observation with a gaussian fit at the velocity and $H\alpha$ strength of the CHVC overplotted (dashed line). The bottom plot shows the sky spectrum with the gaussian fit to the $H\alpha$ detection shown as the dashed line.

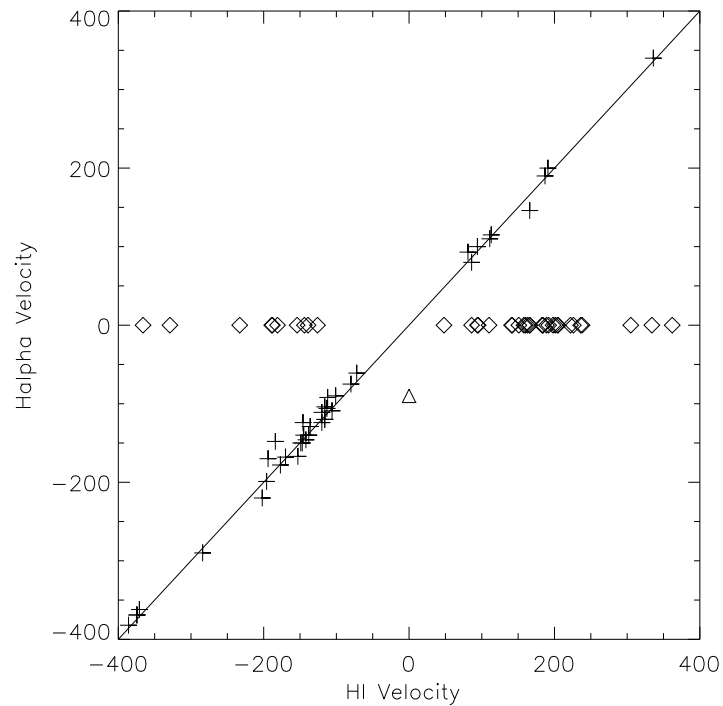


Fig. 2. The relationship between the $H\alpha$ and HI velocity for all of the recently published HVC $H\alpha$ observations (this paper; WW96; T98; B98; T02). Crosses show the detections, diamonds the non-detections in $H\alpha$, and the triangle is the one high-velocity detection in $H\alpha$ but not HI on the edge of Complex M (T98).

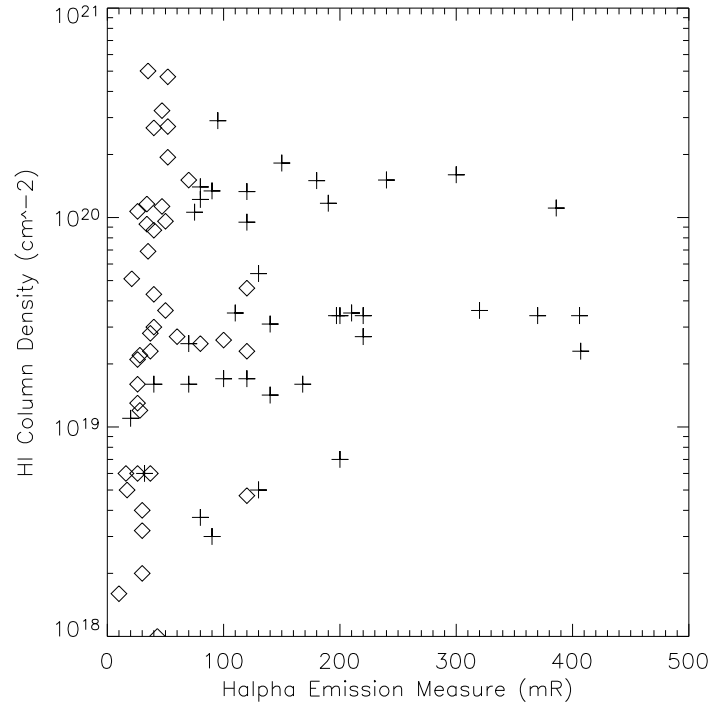


Fig. 3. The relationship between the H α emission measure and the HI column density for the same data shown in Figure 2. Detections are represented by crosses and non-detections are represented by open diamonds. The H α emission measures are NOT extinction corrected. Using the extinction corrected values does not greatly change this plot, as can be noted from the values listed in Table 1 and 2.

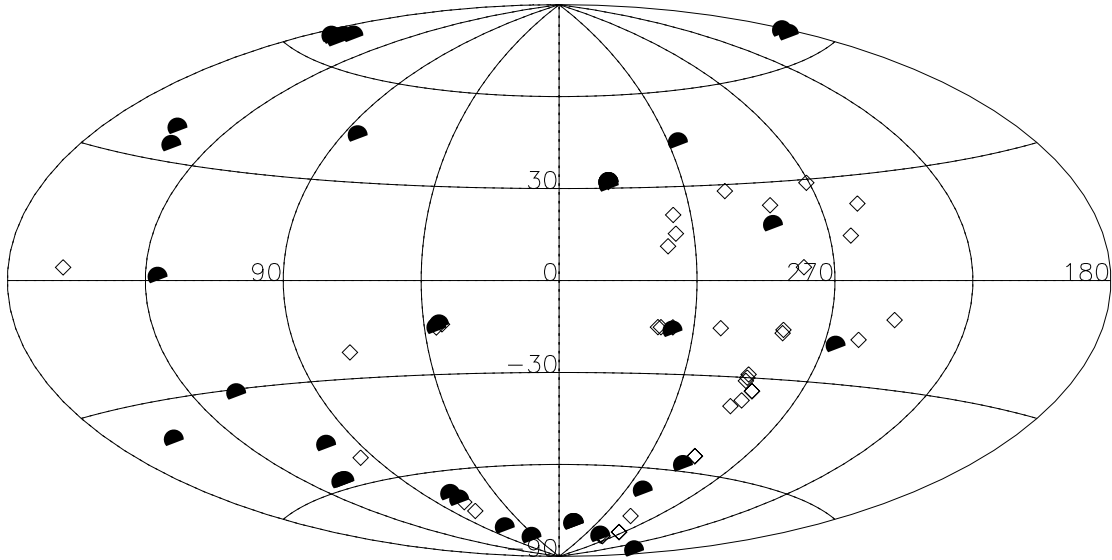


Fig. 4. The distribution of H α detections (solid symbols) and non-detections (open diamonds) of the same data shown in Fig. 2 in Galactic coordinates.

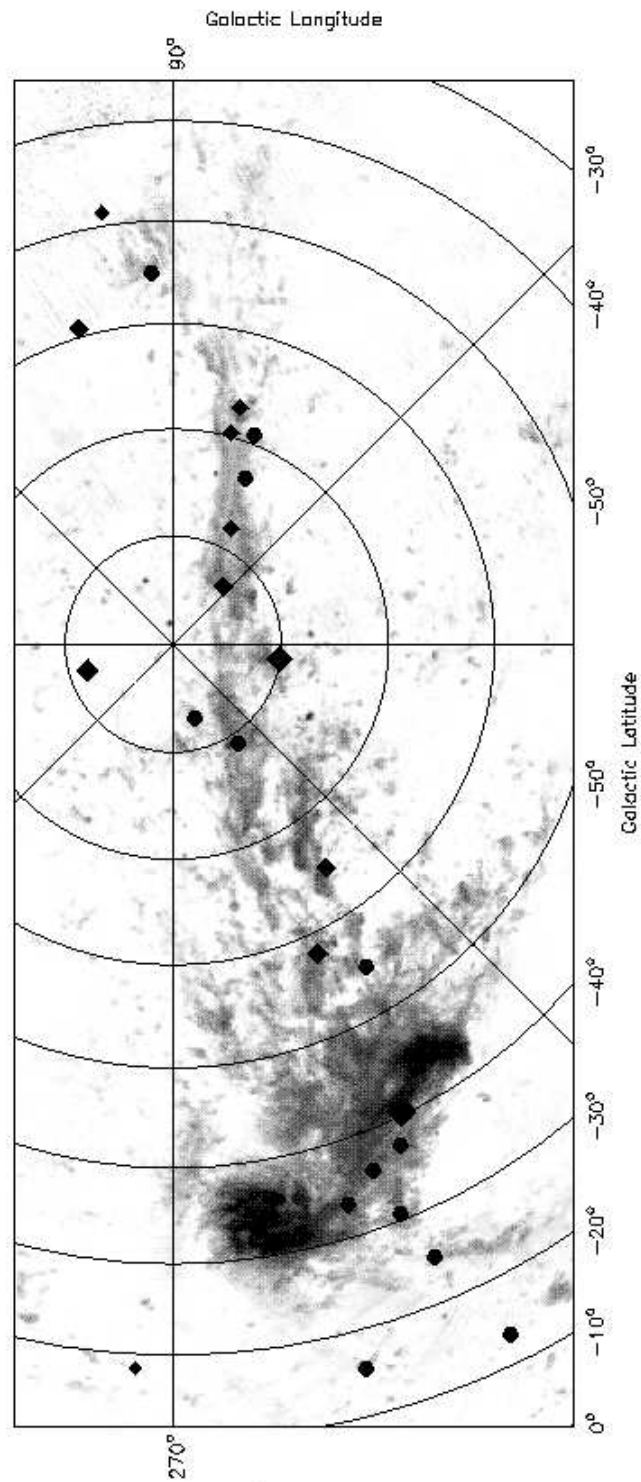


Fig. 5. An HI map of the Magellanic System showing column densities greater than $2 \times 10^{18} \text{ cm}^{-2}$ (P03), with the $\text{H}\alpha$ detections and non-detections labeled as diamonds and circles, respectively. The size of the diamond represents the relative strength of the $\text{H}\alpha$ detection. The positions and strengths of the $\text{H}\alpha$ observations were labeled by eye, and are for general reference only. The detections include this work, the WW96 observations, and two of the CHVCs detected by T02 which are located near the northern tip of the Magellanic Stream.

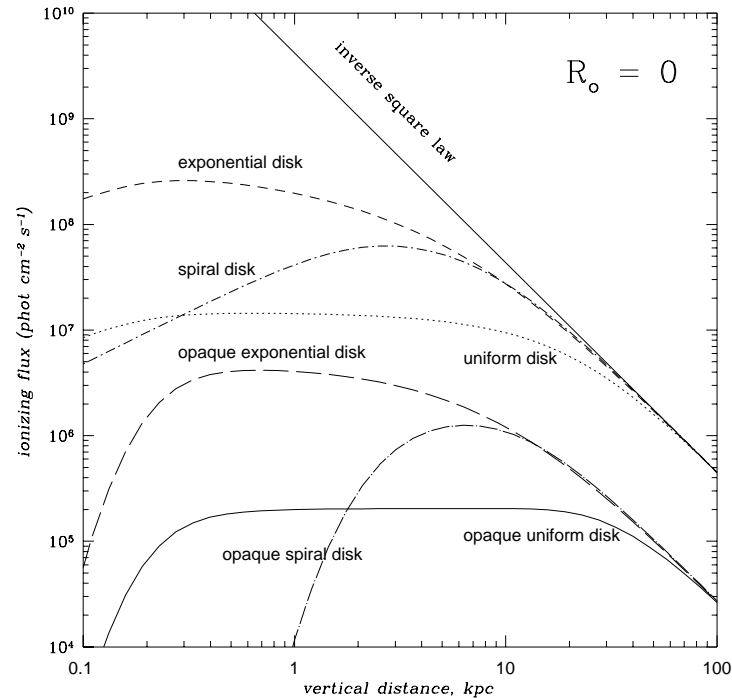


Fig. 6. The halo ionizing flux for different disk distributions (uniform emissivity, exponential and spiral) compared to a simple inverse square law. The vertical distance is measured from the center of the disk along the polar axis. The top three curves are in the absence of dust and converge in the far field limit. The lower three curves include the effects of dust where $\tau_{LL} = 2.8$ ($\hat{f}_{\text{esc}} = 6\%$).

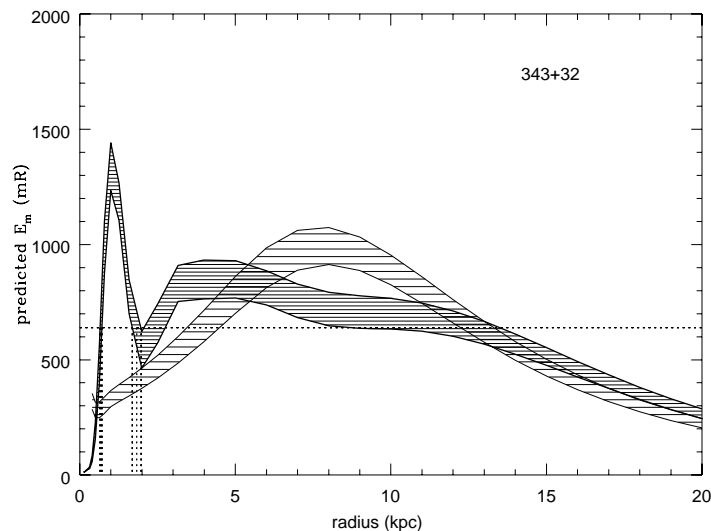


Fig. 7. Predicted run of emission measure (in mR) as a function of radius (in kpc) along our sight line to Complex L. The light shaded model is the $H\alpha$ signal due to an exponential disk of ionizing sources; the dark shading is for the spiral arm model. The horizontal line shows our brightest observed E_m for Complex L. Note the spiral arm model can produce multiple solutions depending on the location of the HVC above the Galaxy. [We note that Weiner *et al.* (2001) detect emission measures of ~ 1 R for a different cloud in Complex L, indicating the near field solution (above a spiral arm) is correct.] Plots of the model predictions for the other detected HVCs can be found at ftp://www.aao.gov.au/pub/local/jbh/disk_halo.

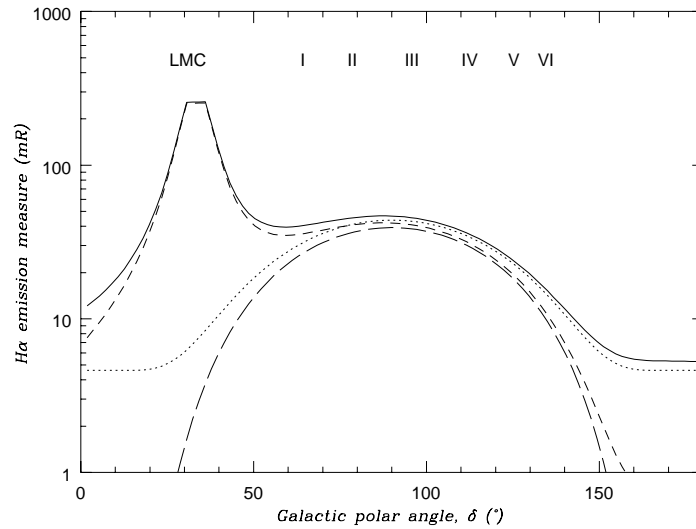


Fig. 8 The predicted H α emission measure along the Stream as a function of polar angle δ in units of log(mR) where $\delta = 90^\circ$ is the South Galactic Pole. The roman numerals refer to the specific Magellanic Stream complex defined by Mathewson et al. (1977). See P03 for the definitions of these complexes on the map shown in Figure 5. The short dashed curve includes the contribution of the LMC; the dotted curve includes the contribution of a UV-bright stellar bulge. The solid curve includes the effect of the LMC and a stellar bulge.

TABLE OF H α EMISSION LINE RESULTS, HI PROPERTIES, AND DISTANCES TO DETECTED HVCs

| Obs. ℓ b | Common ^a Name | N_{HI} (10^{19} cm ⁻²) | V_{lsr} (Hi) | ΔV^b km s ⁻¹ | E_m^c (mR) | $E_{m(obs)}^d$ (mR) | [NII]/H α | V_{lsr} (H α) | D_{mod}^e (kpc) |
|--------------------|---------------------------------|--|-------------------|------------------------------------|-----------------|------------------------|------------------|----------------------------|----------------------|
| 295.1-57.8 | MS I (Fairall 9) | 9.5 | 191 | 52 | 128(D) | 120* | < 0.25 | 200 | 0.5 - 25.7 |
| 304.0-68.3 | MS Ib | 29.0 | 81 | 35 | 99 | 95 | < 0.30 | 93 | 0.5 - 33.2 |
| 342.6-79.6 | MS IIa | 11.1 | -120 | 37 | 407 | 386 | 0.15 | -124 | 1.7 - 9.7 |
| 342.2-79.9 | MS IIa | 3.4 | -116 | 34 | 228(D) | 220 | < 0.18 | -116 | 0.8 - 19.9 |
| 297.5-42.5 | Bridge M | 98.3 | 166 | 66 | 3796 | 3240 | 0.05 | 146 | - |
| 040.3-15.1 | Smith2 ^f | 16.0 | 86 | 38 | 450 | 300 | 0.60 | 80 | 1.2 - 12.7 |
| 040.6-15.5 | Smith1 ^f | 15.1 | 94 | 47 | 360 | 240 | 0.60 | 100 | 1.2 - 13.4 |
| 130.8+00.9 | Complex H ^g | 18.2 | -200 | 16 | 3697 | 150 | - | -170 | - |
| 170.9+64.7 | Complex M W6 | - | - | - | 150 | 140* | - | -90 | 1.7 - 9.6 |
| 163.3+66.7 | Complex M W2 | 11.7 | -101 | 43 | 203 | 190* | - | -90 | 2.2 - 6.7 |
| 341.8+31.3 | Complex L2 ^h | 1.6 | -146 | 58 | 263 | 168 | 2.5 | -124 | 0.5 - 19.9 |
| 343.2+32.1 | Complex L3 | 3.6 | -136 | 36 | 499 | 320 | 2.7 | -129 | 0.6 - 15.2 |
| 343.1+32.0 | Complex L4 | 3.4 | -142 | 41 | 309 | 197 | 2.5 | -146 | 0.6 - 19.0 |
| 343.2+31.9 | Complex L5 | 3.4 | -145 | 39 | 637 | 406 | 2.7 | -140 | 0.7 - 11.2 |
| 343.4+32.0 | Complex L6 | 2.3 | -138 | 35 | 639 | 407 | 2.7 | -140 | 0.7 - 11.1 |
| 153.6+38.2 | Complex A ⁱ | 1.3 | -177 | 23 | 108(W) | 90 | - | -178 | 1.6 - 5.0 |
| 084.3+43.7 | Complex C ⁱ | 0.54 | 120 | 15 | 133(W) | 130 | - | -111 | 1.9 - 14.2 |
| 310.9+44.4 | HVC310.5+44.2+187 | 0.37 | 187 | 40 | 99(D) | 80* | 1.3 | 187 | 0.4 - 27.5 |
| 322.0-15.8 | HVC321.7-16.0+113 | 1.7 | 113 | 59 | 125(D) | 100 | < 0.50 | 113 | 0.5 - 18.5 |
| 104.2-48.0 | :HVC104.2-48-168 ⁱ | 0.6 | -170 | 25 | 39(W) | 32 | - | -168 | 1.1 - 27.8 |
| 118.5-58.2 | CHVC118.2-58.1-373 ⁱ | 3.1 | -374 | 28 | 152(W) | 140 | - | -369 | 1.9 - 10.6 |
| 119.2-30.8 | CHVC119.2-31.1-384 ⁱ | 1.1 | -386 | 20 | 24(W) | 20 | - | -382 | 1.3 - 13.2 |
| 158.0-39.0 | CHVC157.7-39.3-287 ⁱ | 0.5 | -284 | 27 | 147(W) | 130 | - | -290 | 1.7 - 4.3 |
| 197.4-81.8 | CHVC197.0-81.8-184 | 2.7 | -184 | 41 | 227(D) | 220 | < 0.30 | -180 | 1.4 - 12.9 |
| 266.0-18.7 | CHVC266.0-18.7+336 | 1.42 | 336 | 31 | 190(D) | 140* | < 0.60 | 336 | 1.2 - 6.1 |
| 285.9+16.6 | XHVC287.6+17.1+111 ^j | 0.7 | 111 | 32 | 241(D) | 180 | - | 111 | 0.8 - 9.9 |

^a MS refers to a Magellanic Stream complex (Mathewson et al. 1977), Smith is also Complex GCP, many objects are named with their catalog name from P02. ^b ΔV at FWHM of HI line. ^c The emission measure in milliRayleighs (mR) has D in parentheses if the result is from the DBS and W if the result is from WHAM. All values are extinction corrected. ^d E_m before the extinction correction. The characteristic detection errors are 10 mR, unless noted with a *. The * indicates that the H α line is within 2 \AA of a skyline and the errors are between 15 - 30 mR. ^e Modeled distance based on E_m , the HVC position and the model described in B02 ($\hat{f}_{esc} = 6\%$ normal to the disk). There is a near and far field solution based on the location of the HVC over the spiral arms. The error on the distance is generally less than 0.5 kpc for the near field solutions and less than 4 kpc for the far field solutions and this incorporates the difference in using E_m or $E_{m(obs)}$. Exceptions where the errors on the far field solutions are ~ 9 kpc include :HVC104.2-48-168 and CHVC119.2-31.1-384. Plots of the model predictions and specific error values can be found at ftp://www.aao.gov.au/pub/local/jbh/disk_halo. ^f Results published in B98. ^g Unable to model distance because of location in Galactic Plane. The dust correction may not be applicable at such low latitudes. ^h Weighted average for Complex L is $E_{m(obs)}=300$ mR, [NII]/H α = 2.7, $V_{lsr} = -140$. ⁱ Emission line results from T98 and T02. ^j Velocity of this cloud places [NII] λ 6583 right on a skyline.

TABLE OF H α EMISSION LIMITS AND HI PROPERTIES OF UNDETECTED HVC POSITIONS

| Obs. ℓ b | Common ^a Name | N_{HI} (10^{19} cm ⁻²) | V_{lsr} (HI) | ΔV^b km s ⁻¹ | E_m^c (mR) | $E_m(obs)^d$ (mR) | V_{lsr} (H α) |
|--------------------|-----------------------------------|--|-------------------|------------------------------------|-----------------|----------------------|----------------------------|
| 293.4-56.4 | MS I | 3.6, 9.6 | 226, 158 | 23, 40 | < 59, < 54 | < 55*, < 50 | 226, 158 |
| 342.2-79.9 | MS IIa | 3.4 | -116 | 34 | < 52[OIII] | < 52[OIII] | -116 |
| 096.5-53.9 | MS V | 4.6 | -366 | 45 | < 153 | < 120* | -366 |
| 292.4-40.1 | Bridge1 | 50.1 | 184 | 53 | < 42 | < 35* | 184 |
| 290.2-37.6 | Bridge2 | 47.0 | 198 | 74 | < 79 | < 52* | 198 |
| 287.7-34.8 | Bridge3 | 26.8 | 204 | 41 | < 52 | < 40* | 204 |
| 291.7-32.0 | Lead Arm1 | 27.2 | 222 | 33 | < 71 | < 52* | 222 |
| 291.7-30.6 | Lead Arm2 | 19.4 | 236 | 43 | < 78 | < 52* | 236 |
| 292.1-29.7 | Lead Arm3 | 5.1 | 305 | 37 | < 30 | < 21* | 305 |
| 287.5+23.0 | Lead Arm4 | 11.3 | 238 | 36 | < 70 | < 47* | 238 |
| 342.5+31.9 | Complex L1 ^e | 0.1 | -126 | 20 | < 65 | < 43 | -126 |
| 248.5-12.2 | Pop EP1 | 0.6 | 334 | 58 | < 56 | < 16* | 334 |
| 262.7+13.5 | Pop EP2 | 1.6 | 160 | 38 | < 41 | < 26 | 160 |
| 280.1+04.0 | Pop EP3 | 6.9 | 163 | 35 | < 128 | < 35 | 163 |
| 271.2+29.4 | Pop EP4 ^e | 0.2 | 184 | 29 | < 39 | < 30* | 184 |
| 326.5-14.6 | HIPASS J1712-64 | 0.4 | 458 | 41 | < 44 | < 30 | 458 |
| 040.6-15.5 | Smith1 | 15.1 | 94 | 47 | < 70[OIII] | < 70[OIII] | 94 |
| 039.3-13.8 | HVC039.3-13.8-233 | 3.1 | -233 | 29 | < 213(D) | < 120 | -233 |
| 259.2-17.2 | HVC259.1-17.2+362 | 0.4 | 362 | 37 | < 171(D) | < 120 | 362 |
| 301.2+27.7 | HVC301.1+27.6+168 | 2.2 | 166 | 34 | < 37 | < 28 | 166 |
| 321.5+20.7 | HVC321.7+20.8+167 | 3.0 | 166 | 36 | < 53 | < 40 | 166 |
| 257.2+22.0 | :HVC257.2+21.9+188 | 3.1 | 188 | 33 | < 93(D) | < 80* | 188 |
| 324.4+10.6 | :HVC324.4+10.6+151 | 4.3 | 151 | 47 | < 167(D) | < 100 | 151 |
| 162.0+02.5 | CHVC161.6+02.7-186 | 1.2 | -180 | 28 | < 980 | < 28 | -180 |
| 284.6-16.1 | CHVC284.9-16.1+205 ^{e,f} | 11.6 | 192 | 33 | < 48 | < 34* | 192 |
| 285.6-83.3 | CHVC286.3-83.5+091 ^{g,h} | 1.3, 0.6 | 86, -144 | 35, 44 | < 26, < 37 | < 26, < 37 | 86, -144 |
| 289.7-83.0 | CHVC290.6-82.8+095 ^{g,h} | 2.1, 1.6 | 95, -147 | 43, 37 | < 26, < 70 | < 26, < 70 | 95, -147 |
| 306.3-16.0 | CHVC305.9-16.1+185 | 2.3 | 183 | 38 | < 61 | < 37* | 183 |
| 321.0+14.9 | CHVC321.1+14.8+113 | 8.7 | 110 | 32 | < 73 | < 17 | 110 |
| 275.2-80.7 | XHVC275.5-80.8-132 | 10.7 | -139 | 82 | < 26 | < 26 | -139 |
| 290.9-76.3 | XHVC294.2-76.1+134 ^h | 2.8, 0.03 | 141, -154 | 43, 15 | < 37, < 30 | < 37, < 30 | 141, -154 |

^a MS refers to a Magellanic Stream complex (Mathewson et al. 1977), Smith is also Complex GCP, most objects are named with their catalog name from P02. ^b ΔV at FWHM of HI line.

^c The emission measure limit in milliRayleighs (mR) has D in parentheses if the result is from the DBS and [OIII] if it is a limit on the [OIII] λ 5007 emission (2σ). All H α limits are extinction corrected. ^d E_m before the extinction correction. The characteristic detection errors are 10 mR, unless noted with a *. The * indicates the H α line is within 2\AA of a skyline and the errors are between 15 - 30 mR. ^e Compromised by Fraunhofer lines from strong moonlight. ^f Also undetected by the DBS. ^g These clouds have been associated with the Sculptor dSph by Carignan et al. (1998). ^h There is also a negative velocity cloud, XHVC288.4-81.8-109, along this sightline.